2014 American Control Conference (ACC)
June 4-6, 2014. Portland, Oregon, USA

# Information Driven Path Planning and Control for Collaborative Aerial Robotic Sensors Using Artificial Potential Functions

A.C. Bellini, W. Lu, R. Naldi and S. Ferrari

*Abstract*— **A path planning and control method based on adaptive potential functions is presented for a group of unmanned aerial vehicles (UAVs) equipped with onboard sensors, and deployed to search and classify multiple targets. The proposed method plans the motion of the UAVs to support a primary sensing objective that, in this case, is to maximize the classification performance of the sensor measurements gathered by the UAVs over time. An adaptive potential function approach originally developed for ground robots is modified and employed as a guidance law for a class of rotary-wing UAVs that must also avoid obstacles located in a three-dimensional workspace. The simulation results show that, by this approach, a single UAV is capable of visiting targets that offer the best tradeoff between distance and measurement information value. Furthermore, simulations involving multiple UAVs deployed to classify the same set of targets show that, by this approach, there emerge a cooperative behavior by which the UAVs can react, as a group, to the targets' classification uncertainties.**

## I. Introduction

In many sensor applications, including robotic mine hunting [1], cleaning [2], and monitoring of urban driving [3], industrial plants [4] or endangered species [5], unmanned aerial vehicles (UAVs) equipped with onboard exteroceptive sensors are deployed to support a primary sensor objective, such as, target classification, localization, and tracking. Because most exteroceptive sensors are characterized by a bounded field-of-view (FOV), or visibility region, target measurements can be obtained only once the FOV intersects the target geometry [6], [7], [8], [9], [10], [11], [12], [13]. Typically, the FOV can be modeled as a bounded subset of a Euclidian space within which the sensor can obtain measurements. The FOV geometry depends primarily on the sensor parameters and environmental conditions, while the FOV position and orientation depends on the position and orientation of the UAV, also referred to as configuration vector. Thus, by defining the FOV in terms of a body frame embedded on the vehicle, the sensor measurements can be planned by planning the path and control of the UAV.

Because rotary-wing UAVs are capable of vertical take-off and landing, and of maneuvering near obstacles, such as buildings or machineries, in order to reach a target, they are commonly implemented for supporting complex sensor missions and applications. As a result, their path must also be planned to avoid collisions with obstacles, and, possibly, other UAVs, while decreasing the distance traveled, time, or fuel consumption. While they can be used for obstacle avoidance and for shortening distance or fuel consumption, existing robot path planning techniques cannot take into account the stochastic sensing objective, or plan the UAV path based on expected target measurements [2], [14], [15]. Furthermore, they cannot be easily modified to take into account prior targets information, which typically is available from past sensor measurements.

Recently, several sensor path planning approaches have been developed to address sensor planning problems for ground sensors, in a two-dimensional workspace with multiple obstacles and targets of known geometries and locations [15], [10], [13], [16]. Cell decomposition and potential field methods have been developed to address sensor planning problems in [15], [10], [13]. An information roadmap method (IRM) inspired by the probabilistic roadmap method (PRM), but applicable to geometric sensor path planning, was also recently developed in [12], [21]. The IRM method generates a roadmap by sampling a probability density function defined based on the sensor's FOV, and the target geometries and information value modeled from prior information, such as geophysical maps and prior sensor measurements. Relative entropy was used to manage a position fixed sensor to track multiple moving targets in [19]. However, in this case, the sensor FOV, and the geometries of targets and obstacles were not considered.

Although they can be combined with a feedback control design via trajectory following, cell decomposition and IRM algorithms typically assume a free-flying robot and, thus, are not easily modified to account for more realistic dynamic constraints, such as those of a rotary-wing UAVs. Artificial potential function methods have been shown very effective at planning both the path and control law of robots and vehicles governed by an accurate dynamic model. Therefore, this paper extends the potential function approach developed in [13] for ground robots to rotary-wing UAVs that are characterized by holonomic dynamic constraints, and more degrees of freedom. The idea is to employ the potential function method in order to obtain a reference trajectory by considering the kinematic model of the aerial vehicle. With this reference at hand, a low-level tracking controller is then employed so as to follow the desired path.

The method developed in this paper is applicable to a class of aerial robots that are deployed in the same workspace to classify multiple targets. Each aerial robot is characterized by different sensor capabilities, and must avoid collisions with other robots, and with fixed or moving obstacles. This

This work was supported by the National Science Foundation under grant ECCS 1028506 and the FP7 European project SHERPA (IP 600958).

A. Bellini and R. Naldi are with DISI, University of Bologna, Italy {annachiara.bellini,roberto.naldi}@unibo.it. W. Lu and S. Ferrari are with LISC, Duke University, Durham, USA {wenjie.lu,silvia.ferrari}@duke.edu.

class of aerial robot can be implemented in a variety of applications, including quadrotors helicopters equipped with vision or thermal cameras, and deployed to monitor urban environments or endangered species [3], [5], or to inspect chemical plants or manufacturing plants [22]. The main goal of the UAV path planning law then is to maximize the sensor classification performance, while minimizing the distance traveled to conserve time and energy.

The adaptive potential field approach developed in [13] is demonstrated on a network of cooperative, heterogeneous UAV-based sensors, because many centralized planning methods are known to loose efficiency when the number of UAVs increases, when moving obstacles are detected online, or when the sensors are heterogenous. The proposed approach reduces the centralized control of multiple robots to multiple problems in which each UAV is controlled in a decentralized manner, and has complete autonomy in planning its control law. Each UAV acts as a rational autonomous intelligent agent, sharing only information about the uncertainty in target classification, and target/obstacle position and geometry.

The paper is organized as follows. Section II describes the mathematical models. The background on adaptive potential field method is reviewed in section III. Section IV describes the sensor planner and controller developed in this paper, and the implementation and simulation results are shown in section V.

## II. Mathematical Models

### A. The Aerial Vehicle Dynamics

The dynamics of a large class of rotary-wing aerial vehicles, including quadrotors and helicopters, can be described by the so called *vectored-thrust* or *thrust-vectoring* approximation (see, among others, [27] and references therein)

$$\begin{aligned} M\ddot{p} &= -u_f R e_3 + M g e_3 \\ \dot{R} &= RS(w) \\ J\dot{w} &= S(Jw)w + u_\tau \end{aligned} \tag{1}$$

where $p = [x_i\ y_i\ z_i]^T \in \mathbb{R}^3$ denotes the position of the center of gravity of the system expressed in an inertial reference frame, $w = [w^x\ w^y\ w^z]^T \in \mathbb{R}^3$ is the angular speed expressed in a body frame attached to the vehicle, $e_3$ is a unit vector defined as $e_3 := [0\ 0\ 1]^T$, $R \in SO(3)$ is the rotation matrix relating vectors in the body frame to vectors in the inertial frame, $M \in \mathbb{R}_{>}0$ and $J \in \mathbb{R}^{3\times3}$ are the mass and the inertia matrix of the system, $u_f \in \mathbb{R}_{\geq 0}$ denotes the control force generated by the aircraft own actuators, $u_\tau \in \mathbb{R}^3$ is the control torque vector and, for a vector $x \in \mathbb{R}^3$,

$$S(x) := \begin{bmatrix} 0 & -x_3 & x_2 \\ x_3 & 0 & -x_1 \\ -x_2 & x_1 & 0 \end{bmatrix}.$$

To model actuator limitations, the control force and torques are required to satisfy some constraints, namely $|u_f| \leq f^U > 0$, $\|u_\tau\| \leq \tau^U > 0$ with $f^U$, $\tau^U$ modeling respectively the maximum attainable force and torques of the specific aerial vehicle.

As pointed out in [27], a number of control strategies have been proposed in literature to address the problem of tracking a desired reference signal. In [28], in particular, a global stabilizing feedback law capable of tracking a desired position $p^r \in \mathbb{R}^3$ and orientation $R^r \in SO(3)$ is proposed. To satisfy the functional controllability of system (1), the references are required to satisfy some constraints. In particular, being the system under-actuated, namely only four control inputs are available to govern the six degrees-of-freedom (d.o.f.) rigid body dynamics, the reference attitude cannot be chosen arbitrarily but a number of constraints have to be satisfied so as to succeed in the desired position tracking objective. In practice, only four d.o.f. can be directly governed, namely the position $p^r \in \mathbb{R}^3$ and the rotation around the unit vector $e_3$, which in the following will be parameterized by means of the angle $\theta \in \mathbb{R}$. Adopted from [27], the global stabilizing feedback controller is used as low level controller, in order to regulate the UAV with the inputs from the sensor planner. A simplified UAV model is introduced next and is used in the sensor planner.

### B. The Planning and Navigation Scenario

This paper considers the problem of integrated navigation and control for $r$ UAVs equipped with sensors deployed to classify multiple targets in an environment populated with obstacles and possibly other robotic sensors. Every UAV is assumed to have autonomous computing and wireless communication capabilities. Wireless communication is used to share current knowledge about the targets and the obstacles between the UAVs and a central station (which could also be one of the UAVs). However, the UAVs do not communicate or coordinate any decisions on path planning, control, or target assignment. Also, every UAV considers other UAVs as moving obstacles to avoid, and is characterized by a platform geometry $\mathcal{A}_i = \mathcal{A} \in \mathbb{R}^3$, $i = 1, 2, \ldots, r$. All UAVs are equipped a sensor characterized by the same FOV, denoted by $\mathcal{S}_i = \mathcal{S} \in \mathbb{R}^3$, for $i = 1, 2, \ldots, r$, but by a different measurement model.

The sensor FOVs are assumed to be compact (closed and bounded) subsets of $\mathbb{R}^3$. Let $I_A$ denote the index set of the robotic platforms. Each sensor is assumed to be fixed on the robot platform, and to explore a common partially-observed workspace denoted by $\mathcal{W}$ to measure and classify multiple geometric targets. The workspace is also assumed to be a compact subset of a three-dimensional Euclidian space, $\mathcal{W} \in \mathbb{R}^3$, and to be populated with $n$ fixed obstacles $B = \{\mathcal{B}_1, \ldots, \mathcal{B}_n\}$, where $\mathcal{B}_i \in \mathbb{R}^3$, and $m$ fixed targets $T = \{\mathcal{T}_1, \ldots, \mathcal{T}_m\}$, where $\mathcal{T}_i \in \mathbb{R}^3$ with $\mathcal{B}_i \cap \mathcal{T}_j = \emptyset$, $\forall\ i \in I_B$ and $j \in I_T$, where $I_B$ and $I_T$ are the index sets of obstacles and targets. Obstacles and targets are also assumed to be fixed and rigid in $\mathcal{W}$, such that every point of $\mathcal{B}_i$, for $\forall\ i \in I_B$, and every point of $\mathcal{T}_j$, $\forall\ j \in I_T$, have a fixed position with respect to a fixed inertial frame $\mathcal{F}_\mathcal{W}$, embedded in $\mathcal{W}$.

Let $\mathcal{F}_{\mathcal{A}_i}$ be a moving Cartesian frame embedded in $\mathcal{A}_i$. Then, every point of $\mathcal{S}_i$ has a fixed position with respect to $\mathcal{F}_{\mathcal{A}_i}$. The configuration $\mathbf{q}_i = [x_i\ y_i\ z_i\ \theta_i] \in \mathbb{R}^3 \times [0\ \pi]$ is

used to specify the position $[x_i,\ y_i,\ z_i]$ and orientation $\theta_i$ of the $i$th $\mathcal{A}_i$ and $\mathcal{S}_i$ with respect to the inertial frame $\mathcal{F}_\mathcal{W}$. As far as the design of the planner and high level control is concerned, UAVs are represented by the same discrete-time second-order dynamic model,

$$\begin{aligned}\mathbf{q}(t+dt) &= \mathbf{q}(t) + \dot{\mathbf{q}}(t)\ dt + 1/2\ \mathbf{u}(t)\ dt^2 + \boldsymbol{\nu}\\ \dot{\mathbf{q}}(t+dt) &= \dot{\mathbf{q}}(t) + \mathbf{u}(t)\ dt + \boldsymbol{\omega};\end{aligned} \tag{2}$$

where $\mathbf{u} \in \mathbb{R}^4$ is the control input, and $\boldsymbol{\nu}$ and $\boldsymbol{\omega}$ are white noises. Note that the above approximated model is just considering the four d.o.f defined in Subsection II-A, as the high level controller will be only in charge of generating a reference trajectory for the low-level control. Let $\mathcal{C}$ denote the space of all possible UAV configurations, such that $\forall\ \mathbf{q}_i \in \mathcal{C},\ \forall\ j \in I_B\ \mathbf{A}_i \cap \mathbf{B}_j = \emptyset$. For simplicity, it is assumed that the configuration space is connected, although this assumption may not hold at all times due to moving obstacles that might temporarily block the way for the UAV. But, if the configuration space is permanently split into unconnected regions, then all regions must be removed from the configuration space except the one where the vehicle is currently deployed.

Then, the path of the $i$th UAV's centroid is defined as a continuous map $\tau_i : [0,1] \rightarrow \mathcal{C}$, with $\mathbf{q}_{i_0} = \tau_i(0)$ and $\mathbf{q}_{i_f} = \tau_i(1)$, where $\mathbf{q}_{i_0}$ and $\mathbf{q}_{i_f}$ are the initial and final configurations, respectively. Since $\mathcal{S}_i$ is mounted on $\mathcal{A}_i$, the path $\tau_i$ determines the targets in $\mathcal{W}$ that can be measured by the sensor mounted on the $i$th UAV, while traveling from $\mathbf{q}_{i_0}$ to $\mathbf{q}_{i_f}$. Let $Q = \{\mathbf{q}_1, \ldots, \mathbf{q}_r\}$ be the set of UAVs' configurations, and $Q_0 = \{\mathbf{q}_{1_0}, \ldots, \mathbf{q}_{r_0}\}$ and $Q_f = \{\mathbf{q}_{1_f}, \ldots, \mathbf{q}_{r_f}\}$ denote the sets of initial and final sensors' configurations, respectively. Then, the set of paths $\Gamma = \{\tau_1, \ldots, \tau_r\}$ determines the targets in $\mathcal{W}$ that can be detected and classified by the UAV network traveling from the corresponding configuration in $Q_0$, to the corresponding configuration in $Q_f$.

It is assumed that the measurement process of every sensor in the network can be modeled by a known joint probability mass function (PMF) obtained from first principles or prior experiments [20], [17], [12], [10]. Let $\mathbf{Z}_i \in \mathcal{Z} \subset \mathbb{R}^r$ denote the sensor measurements from target $\mathcal{T}_i \in T$ that are used to estimate or classify the unknown target state $\mathbf{X}_i \in \mathcal{X} \subset \mathbb{R}^n$. The sensor characteristics, including the sensor mode, environmental conditions, and sensor noise or measurement errors, are grouped in a vector of parameters $\boldsymbol{\lambda}_i \in \mathcal{D} \subset \mathbb{R}^l$. Then, assuming that the targets' state, sensor measurements, and parameters are random vectors, the sensor measurements can be modeled by a joint PMF that typically can be factorized as follows [12], [10],

$$p(\mathbf{Z}_i, \mathbf{X}_i, \boldsymbol{\lambda}_i) = p(\mathbf{Z}_i \mid \mathbf{X}_i, \boldsymbol{\lambda}_i) p(\mathbf{X}_i) p(\boldsymbol{\lambda}_i),\ \forall i \in I_T \tag{3}$$

assuming that $\mathbf{X}_i$ and $\boldsymbol{\lambda}_i$ are independent variables. In this paper, the sensor model represented by (3) is considered to hold for all targets, and to remain constant regardless of measuring distance at all times. Prior information, such as measurements and environmental maps from satellite sensors, is used to estimate the geometry and location of obstacles and targets in $B$ and $T$, where it is assumed that only a portion of the target and obstacle locations are known *a priori*, and the others are sensed online.

The UAVs are deployed to search and classify targets in $\mathcal{W}$, based on partial prior information about the targets' and obstacles' locations and geometries. Additionally, the path planning algorithm must take into account the value of information, for correctly classifying targets that have been detected up to the present time by prior sensor measurements. Once a target $i \in I_T$ is detected, we assume that its location and geometry $\mathcal{T}_i$ become known, but its classification $\mathbf{X}_i$ remains uncertain, due to the random nature of the measurement process (3). Once the $i$th target is measurement by the UAV sensor, its classification is updated based on $\mathbf{Z}_i$ and $\boldsymbol{\lambda}_i$ by the following equation

$$\mathbf{X}_i = \sum_{\mathbf{x}_i \in \mathcal{X}} \sum_{\boldsymbol{\lambda}_i \in \mathcal{D}} p(\mathbf{Z}_i \mid \mathbf{x}_i, \boldsymbol{\lambda}_i) p(\mathbf{x}_i) p(\boldsymbol{\lambda}_i) \tag{4}$$

where $p(\mathbf{x}_i)$ is the prior PMF given the prior information of the $i$th target, and lower-case letters denote the value of the corresponding (upper-case) random variable. The $i$th target's information value, denoted by $V_i$, is the expected benefit of making additional measurements from $\mathcal{T}_i$, and it can be represented by the expected reduction in uncertainty associated with $\mathbf{Z}_i$, conditioned on the sensor model and prior information. The information value is used to construct the adaptive potential function in next section.

## III. Artificial Potential Function for Geometric Sensing

This section begins by introducing the concept of utility of a measurement and expected information value for a future measurement. The C-Target regions of attraction are defined, then the expected information value is mapped to the configuration space $\mathcal{C}$ into an attractive potential directed to these regions. Two repulsive potentials, one for fixed obstacles and one for moving obstacles, are then added to the attractive potential, in order to build a potential function that the robot can autonomously compute locally, given the geometries and locations of targets and obstacles and the current PMF of the targets. Geometries of the vehicle, sensor FOV, targets and obstacles are of great importance to this method and are the main difference from other known potential function methods for planning.

### A. Measurement Utility

Information-driven sensor planning utilizes information theoretic functions to assess the value of a set of sensor measurements. Target classification can be reduced to the problem of estimating one or more random variables from partial or imperfect measurements. Therefore, the utility of future measurements may be represented by the expected information value of possible measurements. If information value is represented by the decrease of uncertainty, i.e. the decrease in information entropy of the PMF that represent the target state, then, knowing the sensor parameter $\boldsymbol{\lambda}_i$ for each

target $\mathcal{T}_i$, and the current PMF of the target classification, $\mathbf{X}_i$, it is possible to assess how useful it would be for the sensor to measure the target, by calculating expected reduction in the target's state entropy. This idea of utility of a measurement is used to build an adaptive potential field integrated with targets' information value, to determine which targets the UAV should measure and consequently to plan the trajectory of the UAV.

### *B. Target Information Value*

Conditional mutual information is a measure of the information value of one random variable about another random variable, where this information is higher when the two random variables are strongly correlated. For example, if the actual target classification $\mathbf{X}_i$, and the measurement $\mathbf{Z}_i$ are two independent random variables, then their conditional mutual information is null. However, due to the underlying nature of sensor measurements, if a sensor is deployed to classify a target, its measurements are always correlated with the target classification variable. Thus, given a sensor mode $\boldsymbol{\lambda}_i$, a possible measurement $\mathbf{Z}_i$ and a target state $\mathbf{X}_i$, we are interested in reducing the uncertainty in $\mathbf{X}_i$ by observing the value of $\mathbf{Z}_i$. Suppose the current information entropy of the target classification $\mathbf{X}_i$ is,

$$H(\mathbf{X}_i) = -\sum_{\mathbf{x}_i} p(\mathbf{x}_i)\log_2[p(\mathbf{x}_i)], \tag{5}$$

then we can measure the reduction in the uncertainty of $\mathbf{X}_i$ brought by a measurement $\mathbf{z}_i$ from the posterior PMF, using the conditional information entropy [23]:

$$H(\mathbf{X}_i|\mathbf{Z}_i) = -\sum_{\mathbf{x}_i}\sum_{\mathbf{z}_i} p(\mathbf{x}_i,\mathbf{z}_i)\log_2[p(\mathbf{x}_i \mid \mathbf{z}_i)]. \tag{6}$$

Furthermore, because in sensor path planning and control we are interested in determining the expected information value of a measurement $\mathbf{z}_i$ prior to obtaining it, the expected information value of the measurement is defined as mutual information i.e.:

$$\begin{aligned} V_i \doteq\ & I(\mathbf{X}_i;\ \mathbf{Z}_i|\boldsymbol{\lambda}_i) \doteq H(\mathbf{X}_i|\boldsymbol{\lambda}_i) - H(\mathbf{X}_i|\mathbf{Z}_i,\boldsymbol{\lambda}_i) \\ =\ & H(\mathbf{X}) \ -\ \sum_{\mathbf{z}_i} p(\mathbf{z}_i|\boldsymbol{\lambda}_i) H(\mathbf{X}|\mathbf{z}_i,\boldsymbol{\lambda}_i). \end{aligned} \tag{7}$$

The expected information value $V_i$ represents the expected the entropy reduction associated with the $i$th target classification $H(\mathbf{X}_i)$ when it is measured. The higher the expected information value, the higher the importance of the target for the sensor.

### *C. Artificial Potential Function*

The potential field method is a robot motion planning method that control robots based on the gradient field of a potential function. The potential function $U$ represents the characteristics of the configuration space, and are constructed by the geometries and locations of the obstacles and targets. Although diverse functions have been utilized to generate $U$ [24], [25], [26], in this paper, the potential function for the $j$th UAV, $U_j$, is a summation of the attractive potential $U_i^a, \forall\ i \in I_T$ generated by the targets, the repulsive potential $U_l^r, \forall\ l \in I_B$ brought by the obstacles, and possibly the repulsive potential $U_k^s, \forall\ k \in I_A \& k \neq j$ from other UAVs. Thus

$$U_j(\mathbf{q}) = \sum_i U(\mathbf{q})_i^a + \sum_l U(\mathbf{q})_l^r + \sum_{k\neq j} U(\mathbf{q})_k^s \tag{8}$$

where $\mathbf{q} = [x\ y\ z\ \theta]^T$ is the $j$th UAV's configuration in $\mathcal{C}$. The gradient of $U_j$ regarding to $\mathbf{q}_j$ is used to design a UAV controller in next section, and is

$$\nabla U_j(\mathbf{q}) = \left[\frac{\partial U_j(\mathbf{q})}{\partial x}\ \frac{\partial U(\mathbf{q})}{\partial y}\ \frac{\partial U(\mathbf{q})}{\partial z}\ \frac{\partial U(\mathbf{q})}{\partial \theta}\right]^T. \tag{9}$$

The repulsive potential $U(\mathbf{q})_l^r$ is defined as

$$U(\mathbf{q})_l^r \ \doteq\ \begin{cases} \frac{1}{2}\eta_1\left(\frac{1}{\zeta_l(\mathbf{q})} - \frac{1}{d_0}\right)^2, & \text{if } \zeta_l(\mathbf{q}) \le d_0 \\ 0, & \text{otherwise} \end{cases} \tag{10}$$

where $\zeta_l(\mathbf{q})$ denotes the distance from the $l$th obstacle to the UAV at $\mathbf{q}$, and $\eta_1$ is a small constant. In [13], the attractive function for $i$th target is defined as

$$U(\mathbf{q})_i^a \doteq \eta_2(1 - \sigma V_i^a e^{-\frac{\zeta_i^t(\mathbf{q})^2}{2\sigma V_i^a}}) \tag{11}$$

where $\zeta_i^t(\mathbf{q})$ denotes the distance from the $l$th obstacle to a UAV at $\mathbf{q}$; $\eta_2$ is a scaling parameter representing the influence of targets; $V_i$ is the information value of the $i$th target; $\sigma$ is the influence parameter which together with $V_i$ and parameter $a$ decides the influence distance of the $i$th target. Let $\zeta_i = \zeta_i^t(\mathbf{q})$, $U(\zeta_i)_i^a$ can also be regarded as a function of $\zeta_i$. As shown in [13], $U_i(\zeta_i)_i^a$ is an increasing function of $\zeta_i$, the influence distance of the $i$th target $\zeta_i = \sqrt{\sigma V_i^a}$. Before new measurements of targets are obtained, the information values of targets can be calculated and are constant. When new measurements are obtained, the PMF of the target classification is updated via Bayesian law, and thus, information values of targets are updated instantly. Therefore, information values are piecewise constants, and at any given moment (10) is differentiable.

One well known limitation of potential field methods is that the UAV can be trapped in local minima when multiple obstacles and targets are populated in the workspace. The local minima are regions where the potential function gradient is null but do not intersect with any C-Target region. This can severely lower the ability of the UAV or the group of UAVs to efficiently reach the C-Target regions. A local minimum is reached by the UAV when the $L2$ norm of (9) is less than a predefined threshold and no new measurement is obtained. In [13], an PRM based local information roadmap was developed to navigate the robotic sensor escaping the local minimum. In this paper, the same algorithm is extended to navigate UAVs. The planner will find an escape route by generating a random subspace $Q \subset \mathcal{C}$, with the requirement that the current configuration $\mathbf{q} \in Q$ and that at least one target $\mathcal{T}_i \in Q$. After $Q$ is generated, a set of milestones are sampled from $Q$. Then, based on these milestones, a PRM roadmap is built starting from $\mathbf{q}$. In this situation, it is

guaranteed that there exists at least one compact subset of $Q$ where the potential function has lower values than the current one, because $\mathcal{CT}_i \cap Q \neq \emptyset$. This approach further guarantees that the UAV will always navigate to a configuration with lower potential, and thus the UAV will eventually reach a target configuration.

## IV. Planning and control

The sensor planning and control method presented in this section considers a single UAV sensor and its control. Considerations on the cooperation of multiple UAVs are presented in the next section. The UAV is controlled by three components: a mode planner that decides UAV's mode, a high level controller that generates references from UAV's current configuration and the decision provided by the planner, and a low level controller that turns these references into control inputs for the UAV. This section focuses on the design of the planner, of the high level controller, and on the integration with the low level control law. The inputs for the low level controller, that has been taken from [27], are sufficiently smooth time reference trajectories obtained by properly interpolating the reference deriving from the high level control law.

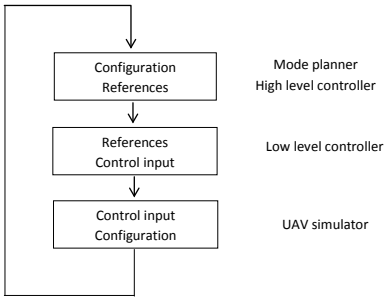


Fig. 1. Three components of the UAV control

### A. Mode Planner

The UAV is equipped with an autonomous planner that is able to compute the adaptive potential function defined in section III at the current configuration. Depending on the value of the gradient potential, the planner can switch between three modes, *gradient navigation mode*, *measuring mode* and *minimum escaping mode*, in order to generate a reference for a low level controller.

When in *gradient navigation mode* (the default mode), the UAV moves with no specifically defined target but only under the effect of the negative gradient of the adaptive artificial potential function. The planner switches to the second mode, *measuring mode*, when the UAV is within a C-Target region. The measuring mode guarantees that UAV stays within the C-Target region long enough for the measurement to be obtained. The third mode, *minimum escaping mode*, is used if UAV gets trapped in a local minimum without measurable targets. In this cases an escape roadmap is computed and the executed. Once the UAV converges to the last milestone $\mathbf{m}_{escape}$, the escaping mode is considered as completed and normal gradient navigation mode resumes.

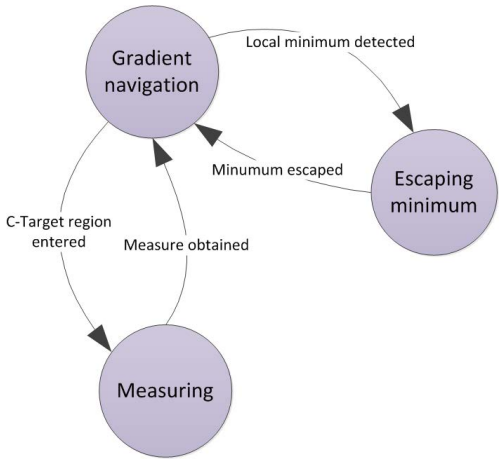


Fig. 2. Planner modes and transitions.

### B. High Level Control

The high level controller considers the UAV's current mode and configuration, and uses the adaptive potential function introduced in the background section to calculate the references for the low level controller. Using a fixed time step $dt$, at time $t$, the reference $\mathbf{q}_j^r(t+dt)$ of the $j$th UAV is obtained by,

$$\mathbf{q}^r(t+dt) = \mathbf{q}_j(t) + \dot{\mathbf{q}}_j(t)dt - \frac{1}{2}\nabla U_j(\mathbf{q}) \otimes [\frac{1}{M} \ \frac{1}{M} \ \frac{1}{M} \ \frac{1}{I}]^T dt^2 \quad (12)$$

where $M$ is the mass of the UAV, $I$ is the robot's moment of inertia around the $z$ axis, and $\mathbf{q}_j(t)$ is the $j$th UAV's configuration at time $t$. The operator $\otimes$ multiplies vectors element-by-element and returns a same size vector. While $\dot{\mathbf{q}}_j(t) = [v_j^x(t) \ v_j^y(t) \ v_j^z(t) \ w_j^z(t)]^T$ where $v_j^x(t)$, $v_j^y(t)$, and $v_j^z(t)$ are the $j$th UAV's velocities in $x$, $y$, $z$ direction respectively, and $w_j^z(t)$ is its angular velocity.

### C. Low Level Control

Goal of the low level control law is to design the control inputs $u_f$ and $u_\tau$ for the dynamical model (1) so as to track a desired position and attitude reference trajectory, as pointed out in Subsection II-A. By considering the nonlinear globally stabilizing controller in [28], the desired references are required to be sufficiently smooth time signals with high order derivatives satisfying appropriate bounds. A trajectory smoother, having as inputs the references $\mathbf{q}_j^r(t)$, can be then employed to obtain time reference signals $p^r(t)$ and $R^r(t)$ fulfilling the assumptions in [28].

## V. Simulation Results

This section focuses on some applications that differ in the number of UAVs deployed a in the sensor's characteristics, exploring the emerging cooperative behavior of the UAVs.

### A. Single UAV

This application explores the behavior of a single UAV equipped deployed in the workspace, with $n$ targets, $m$ fixed obstacles and $r$ moving obstacles. The target states have the

same prior PDF, which can be uniform or not, but all target states are identical at time $t_0$. The sensor parameter $\boldsymbol{\lambda}_i$ (III-B) is supposed to have a fixed value $\boldsymbol{\lambda}_0$ for all targets $\mathcal{T}_i$ in $\mathcal{W}$.

The equality of all target state PDF and the fixed value $S_0$ of the sensor parameter imply that the expected information value of yet unmeasured targets is fixed and equal to a value $V_0$, therefore the attractive potential $U_i^a$ generated by the target $T_i$ depends only on the distance $\rho_i(\mathbf{q})$ of the UAV's current configuration $\mathbf{q}$ to the C-Target region $\mathcal{CT}_i$, with the attractive potential of the closest target generating the strongest virtual attractive force on the robotic sensor. The agent is then attracted to the closest C-Target region, stops there to acquire the measurement, then moves on. When a target has been measured, its information value is set as zero because the uncertainty in the target state cannot be reduced by further measurements of the same sensor.

The UAV is initially deployed at a random location in the workspace. The path followed by the UAV in this case is not generally the shortest path that could be followed and depends strongly on the robot initial configuration. Classification performance depends only on the performance of the sensor. Figure 3 shows the paths followed by a single agent deployed at a random initial location to classify ten randomly placed targets. The simulated sensor has comparable performances for all targets and all target values: a gaussian PDF with a variance $\sigma = 5$, which leads to rather unprecise measurements. Iterations where the location doesn't change are when the agent is sensing the target.

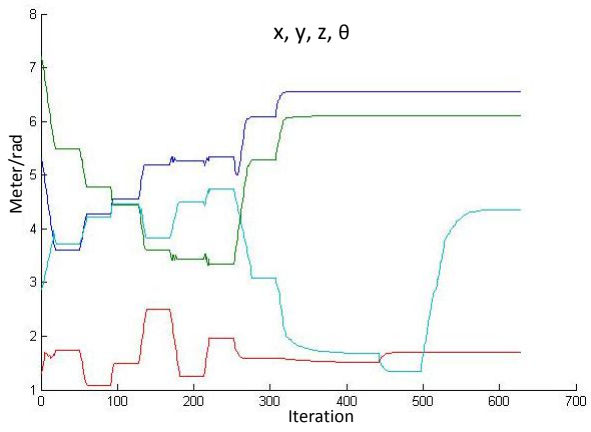


Fig. 3. Path followed by a single agent to classify ten targets.

Figure 4 shows for the same simulation how the global entropy, i.e. the sum of the entropies of the individual targets' PDFs, decreases as measurements are acquired. The initial entropy is $10 \log_2 \|domain\|$, and the rather large residual entropy is due to the large error of the sensor.

### *B. N UAVs with Different Capabilities*

The cooperative aspect emerges more efficiently when the UAVs have different capabilities of sensing, and they have widely different performances for the values in the real target domain. As an example consider a single target $T$; let the

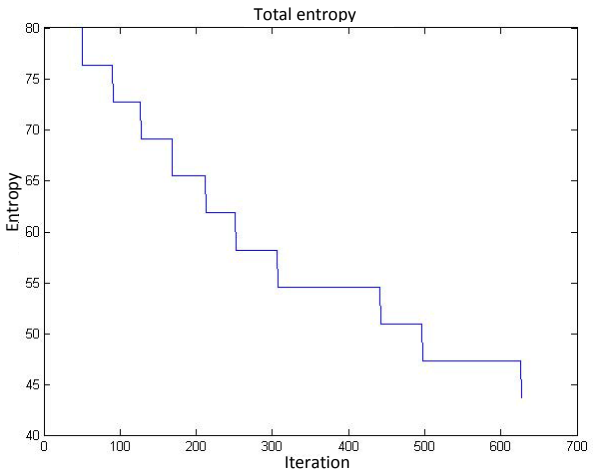


Fig. 4. Global uncertainty decreasing as the measurements are acquired.

target state domain be $[1, \ldots, 256]$ and the prior PDF of $T$ be uniform: $p_X(x_i) = \frac{1}{256}, i = 1 \ldots 256$. Let also the target real value be 19. Two UAVs, $R_{wide}$ and $R_{precise}$, are deployed: $R_{wide}$ has the same performance over the whole domain: it measures the correct value $x_i$ with a normal PDF with $\mu = x_i, \sigma = 5$. It's the same sensor parameters used in the single UAV example and, as seen, has a very low precision. $R_{precise}$ has peak performances in a narrow range of the domain, the $[5, \ldots, 25]$, where it can measure the correct value $x_i$ with a normal PDF defined by $\mu = x_i, \sigma = 0.1$. In the rest of the domain the sensor could indifferently read any value, including the ones in the preferred range.

When the target PDF is still uniform, and its entropy is maximum, with the given parameters the UAV $R_{wide}$ has an expected entropy value $H_{wide}$ that is uniform and shown in blue Fig. 5. The slopes at the ends of the domain are due to border effects.

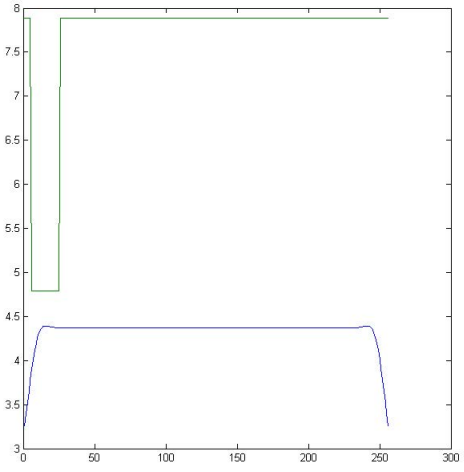

Fig. 5. Uniform expected entropy.

The green line in Fig. 5 shows the expected entropy value $H_{precise}$ when the target PDF is uniform. The rather high residual entropy even in the sensor's range is due to the range

values be possible even for out-of-range measurements. The slight decrease in the uncertainty even for out-of-range values reflects the fact that range values are much more likely to be correct.

These expected entropies are dot-multiplied by the target PDF, which is uniform and $= 1/256$ for each domain value, then the two corresponding expected information values are:

$$V_{wide} = 3.6741,\ V_{precise} = 0.3591$$

The attractive potential on the $R_{wide}$ agent is ten times the attractive potential on the precise sensor; the precise sensor will tend to move very slowly, will mostly try to avoid obstacles passing by, while the wide-spectrum sensor will rush to give a first rough classification of the target.

Once the $R_{wide}$ sensor senses the target, sensing for instance 15 instead of the correct value 19. The target PDF is no longer uniform, as shown in Fig. 6

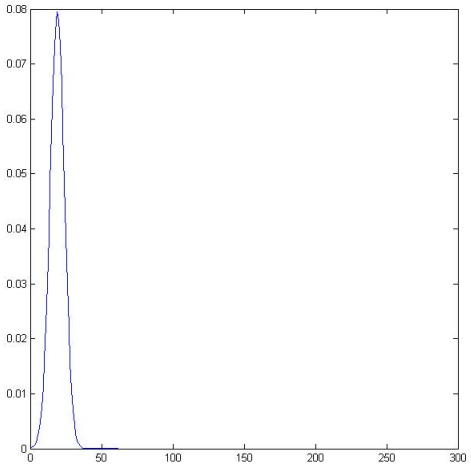


Fig. 6. The target state after the first measurement. Real value is 19, predicted value is 15

The expected information values now change, making $V_{wide} = 0$ and $V_{precise} > 0$. The wide-spectrum sensor is no longer attracted and the precise sensor is attracted.

Given these considerations, the following scenario is prepared and tested: $N$ targets are setup in the workspace, with some obstacles. A number of UAVs are supposed to have a measurement range that covers the whole target state domain, but with low precision. A measurement by any of these UAVs could have a large error, but sufficient to identify the target state.

In the same workspace, other UAVs are also deployed, that can sense only a small range of values but with high precision. When the algorithm is initialized and uncertainty in the target states is maximum, these specialized robots are affected by very small expected information values and therefore moved by very small attractive forces, whereas they can be pushed away by other moving obstacles. As long as these conditions persist, the specialized robots tend then to move very little and slowly, while the general purpose UAVs start to move rapidly to perform a first, rough classification of targets.

As one target $\mathcal{T}_i$ is measured by a general purpose UAV, its target state uncertainty decreases, concentrating in a peak in the range around the real target value. When the PDF is updated to reflect this peak, if there is a UAV $R_j$ specialized in the most likely range, the expected information value for this robotic sensor will actually increase with the reduction of the uncertainty, because the UAVs are able to reduce or almost eliminate the residual uncertainty. Other specialized robotic sensors, that are not tuned to the specific range, will instead compute an even lower expected information value. The robotic sensor $R_j$, affected mostly by the attractive potential of $\mathcal{CT}_i$, will start to navigate toward it, thus maximizing the performance with respect to the distance traveled. Also, if the specialized UAVs almost do not move unless necessary, other UAVs that are planning routes to escape local minima are less likely to replan, improving the performances of the whole class of robots.

Simulations show that this kind of cooperation is possible, however it greatly depends on the accuracy of the precise sensors. Sensors which are completely and uniformly blind outside of their range are not of great utility, because their expected information value doesn't increase easily. Better sensor models, such as sensor that give at least an "out-of-range" measurement instead of a uniform PDF that can also erroneously produce values in the preferred range, could perform better and enhance the cooperative behavior.

### C. Measure A Target Behind A Fixed Obstacle

This situation is set up to test the roadmap method to escape local minima, which becomes of paramount importance as multiple robots are deployed. The workspace is divided in two parts by a wall-obstacle $B_{wall}$, that impedes passage of the robotic sensors except for a single passage. A target $T_{hidden}$ is set on one side of $B_{wall}$ and the UAV are supposed not to be able to obtain measurements from behind the wall. A single UAV is then deployed on the opposite side of $B_{wall}$, in a configuration $\mathbf{q}_0$ from which gradient navigation will bring the UAV to the local minimum that is formed on the side of $B_{wall}$ in the configuration that is closer to $T_{hidden}$. This is the minimum value of the attractive potential function $U_{att}$ that is on the UAV's side of the wall:

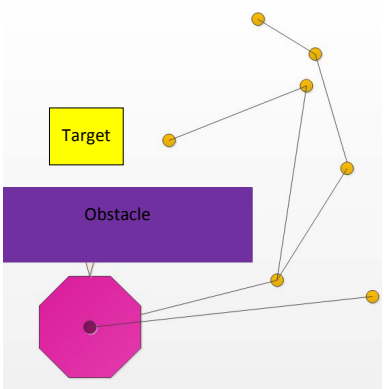


Fig. 7. Robot stuck in a local minimum behind the obstacle.

When the UAV detects the trapping, minimum escaping mode is entered and the milestones are sampled. By construction, the final target milestone has a lower potential than the current configuration, and is located on the opposite side of $B_{wall}$. In this case, the subspace $Q$ used for sampling milestones must include the target configuration or at least a portion of the C-Target region, the current configuration and the passageway left open by the wall. When the sampling is able to sample at least two milestones that are connected by a path that passes through the passageway, a navigation plan from the current minimum to the opposite side of the wall is built, and the robot navigates through the passageway. Simulations with multiple UAVs deployed in the same situation show that the UAVs will pass through the passageway one at a time, provided that the expected information value is large enough. As soon as the information value of the hidden target decreases, UAV will not likely try to reach it.

## VI. Conclusions

The artificial potential function integrated with information value function presented here is an effective method for planning and coordinating UAVs equipped with sensors. It allows to perform independent path-planning and obstacle avoidance, and implicitly provides a mean to maximize the overall performance of a class of UAVs without centralized coordination. Simulation of the different application has shown that the method performs best when the density of UAVs, obstacles and targets is kept low and when the objects are relatively small. As the number of objects increases, the artificial potential function presents many local minima, which require the planner to suspend navigation by gradient and invoke the computationally more expensive roadmap navigation, that however is in line with the overall goal of maximizing classification performance.

## References


[1] R. Siegel, "Land mine detection," *IEEE Instrumentation and Measurement Magazine*, vol. 5, no. 4, pp. 22–28, 2002.

[2] C. Hofner and G. Schmidt, "Path planning and guidance techniques for an autonomous mobile cleaning robot," *Robotics and Autonomous Systems*, vol. 14, pp. 199–212, 1995.

[3] S. Ferrari, C. Cai, R. Fierro, and B. Perteet, "A multi-objective optimization approach to detecting and tracking dynamic targets in pursuit-evasion games," in *Proc. of the 2007 American Control Conference*, New York, NY, 2007, pp. 5316–5321.

[4] D. Culler, D. Estrin, and M. Srivastava, "Overview of sensor networks," *Computer*, vol. 37, no. 8, pp. 41–49, 2004.

[5] P. Juang, H. Oki, Y. Wang, M. Martonosi, L. Peh, and D. Rubenstein, "Energy efficient computing for wildlife tracking: Design tradeoffs and early experiences with zebranet," *Proc. $10^th$ International Conference on Architectural Support for Programming Languages and Operating Systems (ASPLOS-X)*, 2002.

[6] S. Y. Chen and Y. F. Li, "Automatic sensor placement for model-based robot vision," *IEEE Transactions on Systems, Man, and Cybernetics - Part B*, vol. 34, no. 1, pp. 393–408, 2004.

[7] S. Chen and Y. Li, "Vision sensor planning for 3cd model acquisition," *IEEE Transactions on Systems, Man, and Cybernetics - Part B*, vol. 35, no. 5, pp. 894–904, 2005.

[8] H. Choset, "Coverage for robotics: A survey of recent results," *Annals of Mathematics and Artificial Intelligence*, vol. 31, no. 1-4, pp. 113–126, 2001.

[9] K. Baumgartner and S. Ferrari, "A geometric transversal approach to anayzing track coverage in sensor networks," *IEEE Transactions on Computers*, vol. 57, no. 8, 2008.

[10] C. Cai and S. Ferrari, "Information-driven sensor path planning by approximate cell decomposition," *IEEE Transactions on Systems, Man, and Cybernetics - Part B*, vol. 39, no. 3, pp. 672–689, 2009.

[11] S. Ferrari, R. Fierro, B. Perteet, C. Cai, and K. Baumgartner, "A geometric optimization approach to detecting and intercepting dynamic targets using a mobile sensor network," *SIAM Journal on Control and Optimization*, vol. 48, no. 1, pp. 292–320, 2009.

[12] G. Zhang, S. Ferrari, and M. Qian, "Information roadmap method for robotic sensor path planning," *Journal of Intelligent and Robotic Systems*, vol. in press, 2009.

[13] G. Zhang and S. Ferrari, "An adaptive artificial potential function approach for geometric sensing," in *Proc. of IEEE International Conference on Decision and Control*, Shanghai, China, 2009, pp. 7903–7910.

[14] E. U. Acar, "Path planning for robotic demining: Robust sensor-based coverage of unstructured environments and probabilistic methods," *International Journal of Robotic Research*, vol. 22, 2003.

[15] S. Ferrari and C. Cai, "Information-driven search strategies in the board game of clue," *IEEE Transactions on Systems, Man, and Cybernetics - Part B*, vol. 39, no. 3, pp. 607–625, 2009.

[16] C. Cai and S. Ferrari, "Comparison of information-theoretic objective functions for decision support in sensor systems," in *Proc. American Control Conference*, New York, NY, 2007, pp. 63–133.

[17] F. Zhao, J. Shin, and J. Reich, "Information-driven dynamic sensor collaboration," *IEEE Signal Processing Magazine*, vol. 19, pp. 61–72, 2002.

[18] W. Schmaedeke, "Information based sensor management," in *Proc. of SPIE Signal Processing, Sensor Fusion, and Target Recognition II*, vol. 1955, Orlando, FL, 1993, pp. 156–164.

[19] C. Kreucher, K. Kastella, and A. Hero, "Sensor management using an active sensing approach," *Signal Processing*, vol. 85, pp. 607–624, 2005.

[20] K. Kastella, "Discrimination gain to optimize detection and classification," *IEEE Transactions on Systems, Man, and Cybernetics - Part A*, vol. 27, no. 1, pp. 112–116, 1997.

[21] M. Qian and S. Ferrari, "Probabilistic deployment for multiple sensor systems," in *Proc. of the $12^th$ SPIE Symposium on Smart Structures and Materials: Sensors and Smart Structures Technologies for Civil, Mechanical, and Aerospace Systems*, vol. 5765, San Diego, 2005, pp. 85–96.

[22] R. Haarbrink and E. Koers, "Helicopter uav for photogrammetry and rapid response," in *2nd Int. Workshop" The Future of Remote Sensing", ISPRS Inter-Commission Working Group I/V Autonomous Navigation*, vol. 36, 2006, p. 1.

[23] Shannon, C. *A mathematical theory of communication* The Bell System Technical Journal, vol 27, pp 379-423, 623-656, 1948.

[24] J. Ren and K. Mclsaac, "A hybird-systems approach to potential field navigation for a multi-robot team," in *Proc. of IEEE International Conference on Robotics and Automation*, Taipei, Taiwan, 2003, pp. 3875–3880.

[25] S. Shimoda, Y. Kuroda, and K. Iagnemma, "Potential field navigation of high speed unmanned ground vehicles on uneven terrain," in *Proc. of IEEE International Conference on Robotics and Automation*, Barcelona, Spain, 2005, pp. 2839–2844.

[26] S. Ge and Y. Cui, "New potential functions for mobile robot path planning," *IEEE Transactions on Robotics and Automation*, vol. 16, no. 5, 2000.

[27] M. Hua, T. Hamel, P. Morin and C. Samson, "Introduction to Feedback Control of Underactuated VTOL Vehicles," in *IEEE Control Systems Magazine*, vol. 33, no. 2, 2013, pp. 61–75.

[28] R. Naldi, M. Furci, R.G. Sanfelice and L. Marconi, "Global Trajectory Tracking for Underactuated VTOL Aerial Vehicles using a Cascade Control Paradigm," in *Proc. of IEEE Conference on Decision and Control*, to appear, 2013.